Production behaviour and electromagnetic form factors of Λ_c

Weiping Wang (On behalf of BESIII Collaboration)

May 4th, 2017

Outline

- Introduction
- Data sets and analysis method
- Systematic uncertainty
- Total cross section
- Angular distribution study
- Summary

Baryon form factor

- One of the most challenging questions in contemporary physics is why and how quarks are confined into hadrons.
- The study of hadron electric and magnetic structures can provide a key.
- The electromagnetic form factors (EMFFs) have been a powerful tool in understanding the structure of nucleons.

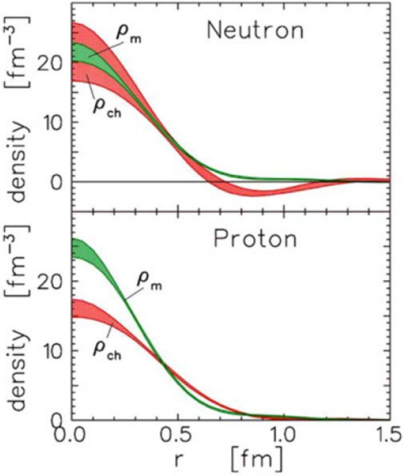

EMFF: Sachs form factor G_E and G_M

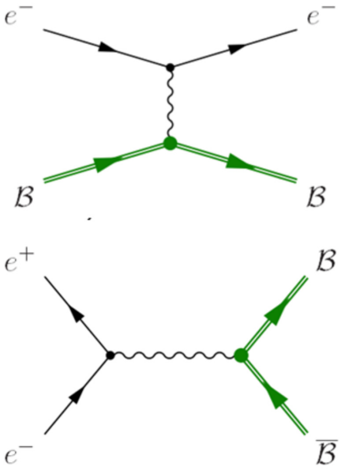

- Space-like:
  - Studied using $e^- B \to e^- B$ scattering.
  - $q^2 = (p^f_{e^-} - p^i_{e^-})^2 < 0$.
  - G_E and G_M are real numbers.
- Time-like:
  - Studied using $e^+e^- \to B\bar{B}$ reaction.
  - $q^2 = (p_{e^+} + p_{e^-})^2 > 0$.
  - G_E and G_M are complex.

EMFF: Sachs form factor G_E and G_M

- The nucleon electromagnetic current $\mathcal{J}^\mu$ is described by the nucleon electromagnetic vertex Γ^μ.

$$\Gamma^\mu = F_1(Q^2)\gamma^\mu + \kappa F_2(Q^2)\frac{i\sigma^{\mu\nu}q_\nu}{2m}$$

- The F_1 and F_2 are Dirac and Pauli form factors, and the Sachs form factors are given by

$$G_E = F_1 - \tau\kappa F_2, \qquad G_M = F_1 + \kappa F_2$$

where the $\tau = Q^2/4m^2$ and κ is the anomalous part of the magnetic momentum.

- G_E and G_M can be interpreted as Fourier transforms of spatial distributions of charge and magnetization of the nucleon in the Breit frame

$$\rho(r) = \int \frac{d\vec{k}}{(2\pi)^2} e^{i\vec{k}\cdot\vec{r}} \frac{G_E(k^2)}{\sqrt{1+\frac{k^2}{4m^2}}}$$

Baryon production

The Born cross section of the reaction $e^+e^- \rightarrow \gamma^* \rightarrow B\bar{B}$ can be parameterized in terms of EMFFs:

$$\sigma_{B\bar{B}}(q) = \frac{4\pi\alpha^2 C\beta}{3q^2}[|G_M(q)|^2 + \frac{1}{2\tau}|G_E(q)|^2]$$

- Baryon velocity $\beta = \sqrt{1 - 4m_B^2/q^2}$, $\tau = q^2/4m_B^2$.
- The Coulomb factor C:
  - For neutral B, $C = 1$.
  - For charged B, $C = \varepsilon R$ with $\varepsilon = \frac{\pi\alpha}{\beta}$ and $R = \frac{\sqrt{1-\beta^2}}{1-e^{-\pi\alpha/\beta}}$, which results in a non-zero cross section at threshold.

Baryon production

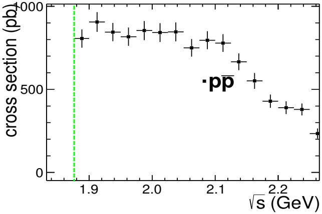

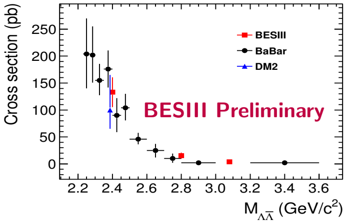

- $e^+e^- \to p\bar{p}$: an enhancement and wide-range plateau.
- $e^+e^- \to \Lambda\bar{\Lambda}$: enhancement near threshold.
- Belle data: not precise enough.
- BESIII can measure $e^+e^- \to \Lambda_c^+\bar{\Lambda}_c^-$ more precisely.
- Drive a further understanding of baryon structure.

BEPCII and BESIII

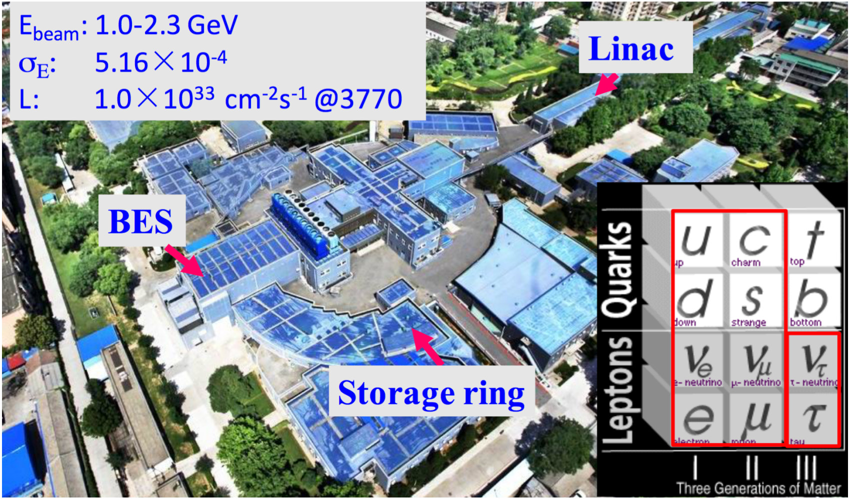

BEPC = Beijing Electron Positron Collider

BEPCII and BESIII

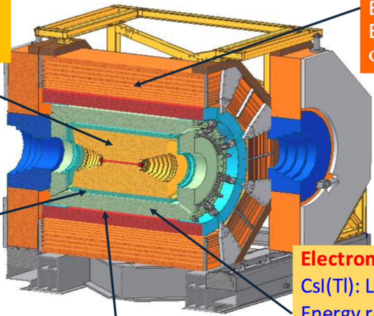

Data sets and tagged modes

Data sample:

$\sqrt{s}$ (GeV)	$\mathcal{L}_{int}$ (pb^{-1})	Energy error
4.5745	47.67	0.72 MeV
4.580	8.545	–
4.590	8.162	–
4.5995	566.9	0.74 MeV

Tagged modes:

Decay modes	Absolute BR(%)	Subsequent BR(%)	Total BR(%)
1. $\Lambda_c^+ \to p^+ K^- \pi^+$	5.84 ± 0.35	–	5.84 ± 0.35
2. $\Lambda_c^+ \to p^+ K_S^0$, $K_S^0 \to \pi^+\pi^-$	1.52 ± 0.09	69.2	1.05 ± 0.06
3. $\Lambda_c^+ \to \Lambda\pi^+$, $\Lambda \to p^+\pi^-$	1.24 ± 0.08	63.9	0.79 ± 0.05
4. $\Lambda_c^+ \to p^+ K^- \pi^+ \pi^0$, $\pi^0 \to \gamma\gamma$	4.53 ± 0.38	98.8	4.48 ± 0.38
5. $\Lambda_c^+ \to p^+ K_S^0 \pi^0$, $K_S^0 \to \pi^+\pi^-$, $\pi^0 \to \gamma\gamma$	1.87 ± 0.14	69.2×98.8	1.28 ± 0.10
6. $\Lambda_c^+ \to \Lambda\pi^+\pi^0$, $\Lambda \to p^+\pi^-$, $\pi^0 \to \gamma\gamma$	7.01 ± 0.42	63.9×98.8	4.43 ± 0.27
7. $\Lambda_c^+ \to p^+ K_S^0 \pi^+\pi^-$, $K_S^0 \to \pi^+\pi^-$	1.53 ± 0.14	69.2	1.06 ± 0.10
8. $\Lambda_c^+ \to \Lambda\pi^+\pi^+\pi^-$, $\Lambda \to p^+\pi^-$	3.81 ± 0.30	63.9	2.43 ± 0.19
9. $\Lambda_c^+ \to \Sigma^0\pi^+$, $\Sigma^0 \to \Lambda\gamma$, $\Lambda \to p^+\pi^-$	1.27 ± 0.09	63.9	0.81 ± 0.06
10. $\Lambda_c^+ \to \Sigma^+\pi^+\pi^-$, $\Sigma^+ \to p\pi^0$, $\pi^0 \to \gamma\gamma$	4.25 ± 0.31	51.6×98.8	2.17 ± 0.16

Analysis strategy

- Intermediate states are selected in advance.
- Minimum ΔE is required in each mode.
- No optimal requirement level between accepting modes.
- The variable M_{BC} is utilized to determine the signal yields.
- Detection efficiencies are obtained by fitting.
- Λ_c^+ and $\bar{\Lambda}_c^-$ are reconstructed independently.
- Total cross section is obtained from weighted average.

Intermediate states

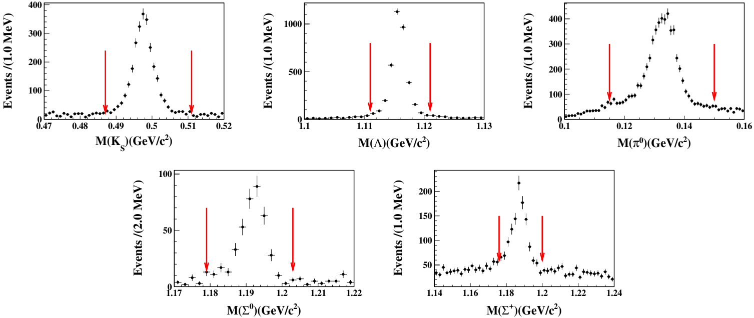

- $M_{\text{Inv.}}$ of intermediate states at $\sqrt{s} = 4.5995\ \mathrm{GeV}$.
- Red arrows indicate signal window.
- Combined data of charge conjugate sector.

Energy difference and beam-constraint mass

$$\Delta E = E - E_{\mathrm{beam}}$$

$$M_{BC} = \sqrt{E_{\mathrm{beam}}^2/c^4 - |\overrightarrow{p}|^2/c^2}$$

- M_{BC} is Beam Constraint (BC) mass.
- E: measured energy of Λ_c candidate.
- $\overrightarrow{p}$: measured momentum of Λ_c candidate.
- E_{beam}: mean value of beam energy.
- Same ΔE cuts for Λ_c^+ and $\bar{\Lambda}_c^-$.
- No additional hadron is produced.
- M_{BC} peaking at the PDG mass of Λ_c.

Mode	ΔE window (GeV)
$pK^-\pi^+$	(-0.02,0.02)
pK_S^0	(-0.02,0.02)
$\Lambda\pi^+$	(-0.02,0.02)
$pK^-\pi^+\pi^0$	(-0.03,0.02)
$pK_S^0\pi^0$	(-0.03,0.02)
$\Lambda\pi^+\pi^0$	(-0.03,0.02)
$pK_S^0\pi^+\pi^-$	(-0.02,0.02)
$\Lambda\pi^+\pi^+\pi^-$	(-0.02,0.02)
$\Sigma^0\pi^+$	(-0.02,0.02)
$\Sigma^+\pi^+\pi^-$	(-0.03,0.02)

Energy difference distribution

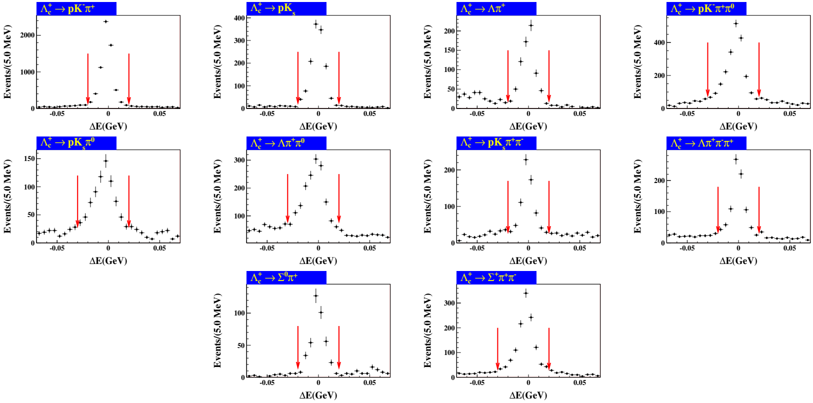

- ΔE of each mode at $\sqrt{s} = 4.5995\ \mathrm{GeV}$.
- M_{BC} cut is applied.
- Red arrows indicate signal window.
- Combined data of charge conjugate sector.

Background study

The background is studied from three aspects:

- Vetoes for same-final-states background.
- M_{BC} distributions in cocktail MC.
- Cross feed between tagged modes.

The veto requirements are determined by studying the data:

modes	Background modes	vetoes
$pK_S^0\pi^0$	$\Lambda\pi^+\pi^0$	veto Λ with $M(p\pi^-)$ lies in (1.100, 1.125) GeV/c^2
	$\Sigma^+\pi^+\pi^-$	veto Σ^+ with $M(p\pi^0)$ lies in (1.170, 1.200) GeV/c^2
$pK_S^0\pi^+\pi^-$	$\Lambda\pi^+\pi^+\pi^-$	veto Λ with $M(p\pi^-)$ lies in (1.100, 1.125) GeV/c^2
$\Lambda\pi^+\pi^+\pi^-$	$pK_S^0\pi^+\pi^-$	veto K_S^0 with $M(\pi^+\pi^-)$ lies in (0.490, 0.510) GeV/c^2
$\Sigma^+\pi^+\pi^-$	$pK_S^0\pi^0$	veto K_S^0 with $M(\pi^+\pi^-)$ lies in (0.490, 0.510) GeV/c^2
	$\Lambda\pi^+\pi^0$	veto Λ with $M(p\pi^-)$ lies in (1.110, 1.120) GeV/c^2

Cocktail MC distribution

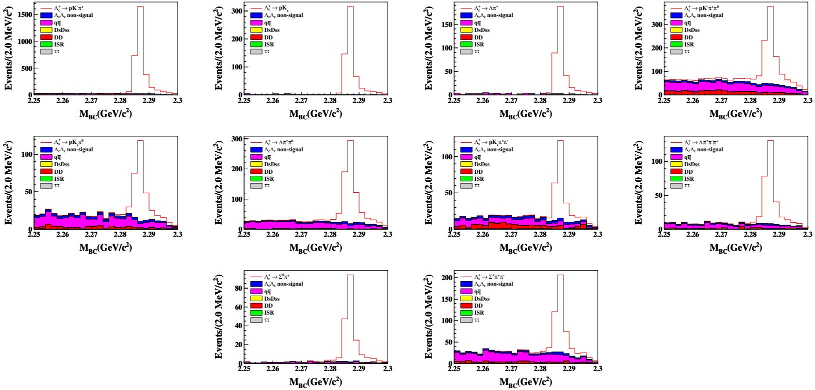

- Inclusive MC generated at 4.600 GeV.
- Sizes of MC samples have been scale to data.
- The background can be described by ARGUS function.

Cross feed estimation

signal modes	Background modes										Total Survived
	$pK^-\pi^+$	pK_S^0	$\Lambda\pi^+$	$pK^-\pi^+\pi^0$	$pK_S^0\pi^0$	$\Lambda\pi^+\pi^0$	$pK_S^0\pi^+\pi^-$	$\Lambda\pi^+\pi^+\pi^-$	$\Sigma^0\pi^+$	$\Sigma^+\pi^+\pi^-$	
$pK^-\pi^+$	261769	10	1	145	23	58	4	30	2	143	263074
pK_S^0	21	49980	23	0	3	4	0	0	7	5	50138
$\Lambda\pi^+$	0	5	29995	1	0	2	0	0	83	0	30269
$pK^-\pi^+\pi^0$	1597	3	3	71151	53	114	68	133	2	148	78110
$pK_S^0\pi^0$	210	22	17	132	21157	343	118	43	15	83	23806
$\Lambda\pi^+\pi^0$	34	3	45	6	96	57844	0	260	838	154	63378
$pK_S^0\pi^+\pi^-$	59	2	1	232	145	45	18472	402	4	45	21507
$\Lambda\pi^+\pi^+\pi^-$	3	0	2	14	2	179	33	23176	1	5	24694
$\Sigma^0\pi^+$	0	0	119	0	0	37	0	0	16086	0	16615
$\Sigma^+\pi^+\pi^-$	531	38	3	165	99	322	42	161	19	33334	37015
Total Generated	509030	89999	71591	418112	116115	416653	90768	218187	69165	182799	–

signal modes	Background modes									
	$pK^-\pi^+$	pK_S^0	$\Lambda\pi^+$	$pK^-\pi^+\pi^0$	$pK_S^0\pi^0$	$\Lambda\pi^+\pi^0$	$pK_S^0\pi^+\pi^-$	$\Lambda\pi^+\pi^+\pi^-$	$\Sigma^0\pi^+$	$\Sigma^+\pi^+\pi^-$
1. $pK^-\pi^+$	99.5	0.0	0.0	0.1	0.0	0.0	0.0	0.0	0.0	0.1
2. pK_S^0	0.0	99.7	0.0	0.0	0.0	0.0	0.0	0.0	0.0	0.0
3. $\Lambda\pi^+$	0.0	0.0	99.1	0.0	0.0	0.0	0.0	0.0	0.3	0.0
4. $pK^-\pi^+\pi^0$	2.0	0.0	0.0	91.1	0.1	0.1	0.1	0.2	0.0	0.2
5. $pK_S^0\pi^0$	0.9	0.1	0.1	0.6	88.9	1.4	0.5	0.2	0.1	0.3
6. $\Lambda\pi^+\pi^0$	0.1	0.0	0.1	0.0	0.2	91.3	0.0	0.4	1.3	0.2
7. $pK_S^0\pi^+\pi^-$	0.3	0.0	0.0	1.1	0.7	0.2	85.9	1.9	0.0	0.2
8. $\Lambda\pi^+\pi^+\pi^-$	0.0	0.0	0.0	0.1	0.0	0.7	0.1	93.9	0.0	0.0
9. $\Sigma^0\pi^+$	0.0	0.0	0.7	0.0	0.0	0.2	0.0	0.0	96.8	0.0
10. $\Sigma^+\pi^+\pi^-$	1.4	0.1	0.0	0.4	0.3	0.9	0.1	0.4	0.1	90.1

- All cross feed rates are less than 2% and typically are about 1%.

Yields

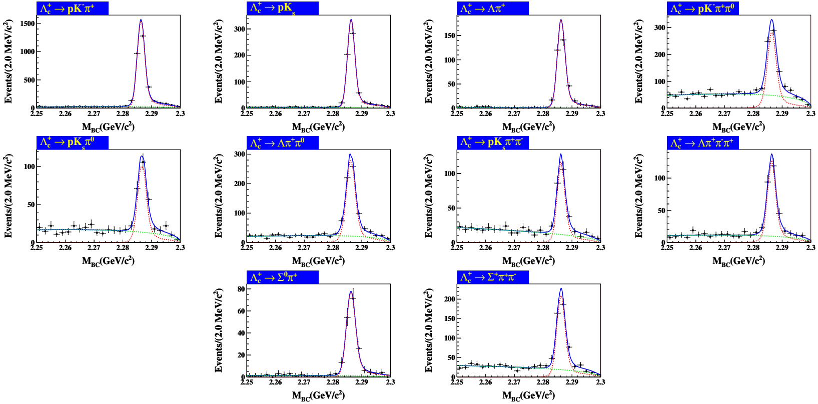

- Un-binned maximum likelihood fits.
- Signal shape function = Signal MC shape $\otimes$ Gaussian function.
- Background function = ARGUS function.
- Parameters of Gaussian and ARGUS function are **free** at 4.5995 GeV.

Yields

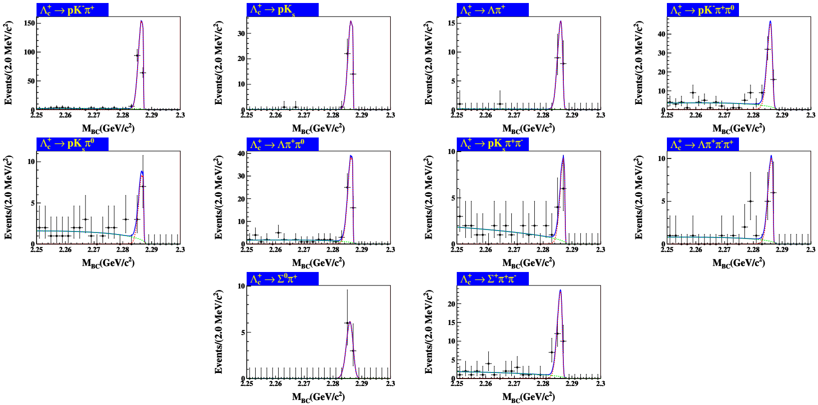

- Fit results at $\sqrt{s} = 4.5745$ GeV.
- Parameters of Gaussian and ARGUS function are **fixed**.
- Similar procedures at $\sqrt{s} = 4.580$ and 4.590 GeV.

Detection efficiencies

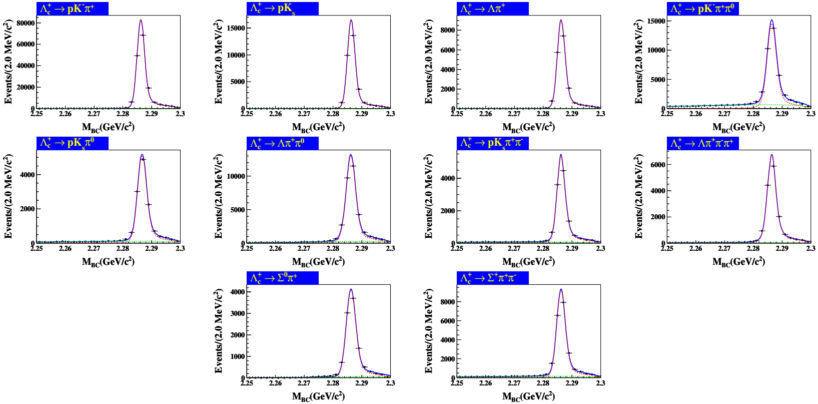

- Efficiencies are obtained by fitting the M_{BC} of signal MC.
- A similar fit as performed on data.
- All parameters of Gaussian and ARGUS function are **free**.
- ΔE and M_{BC} resolution correction on signal MC before fitting.

Results

Mode	$N^{data}_{\Lambda_c^+}$	$\varepsilon_{\Lambda_c^+}$ (%)	$N^{data}_{\bar{\Lambda}_c^-}$	$\varepsilon_{\bar{\Lambda}_c^-}$ (%)
1. $pK^-\pi^+$	2967 ± 60	51.1	3215 ± 60	51.2
2. pK^0_S	620 ± 26	55.5	622 ± 26	55.7
3. $\Lambda\pi^+$	354 ± 19	41.7	345 ± 20	42.2
4. $pK^-\pi^+\pi^0$	654 ± 36	14.3	721 ± 37	15.2
5. $pK^0_S\pi^0$	228 ± 19	17.1	251 ± 18	17.6
6. $\Lambda\pi^+\pi^0$	640 ± 31	13.1	631 ± 31	13.5
7. $pK^0_S\pi^+\pi^-$	231 ± 18	19.4	193 ± 17	19.4
8. $\Lambda\pi^+\pi^+\pi^-$	273 ± 20	11.4	254 ± 19	11.2
9. $\Sigma^0\pi^+$	175 ± 14	22.2	216 ± 15	23.3
10. $\Sigma^+\pi^+\pi^-$	442 ± 26	17.2	364 ± 24	17.3

- Results at 4.5995 GeV.
- Extracted in signal region (2.276, E_{beam}) GeV/c^2.
- Efficiencies do not include any subsequent BRs.

Systematic uncertainty (I): Mode specific

- (Tracking) PID efficiencies are weighted with (transverse) momentum.
- K_S^0 and Λ reconstruction uncertainty with tracking and PID uncertainties of the decay daughter included.
- systematic uncertainty of reconstructing π^0.
- MC statistical uncertainty.
- MC signal modeling uncertainty.
- Uncertainty of subsequent BRs and absolute BRs.

Mode	Tracking	PID	K_S^0	Λ	π^0	MC stat.	Signal model	Sub. BR.	Abs. BR.	Total
1. $pK^-\pi^+$	3.2	4.6	–	–	–	0.2	–	–	6.0	8.2
2. pK_S^0	1.3	0.5	1.2	–	–	0.6	0.2	0.1	5.6	5.9
3. $\Lambda\pi^+$	1.0	1.0	–	2.5	–	0.8	0.5	0.8	6.1	6.9
4. $pK^-\pi^+\pi^0$	3.0	7.6	–	–	1.0	0.6	2.0	–	8.3	11.9
5. $pK_S^0\pi^0$	1.0	1.8	1.2	–	1.0	1.1	1.0	0.1	7.5	8.0
6. $\Lambda\pi^+\pi^0$	1.0	1.0	–	2.5	1.0	0.6	0.6	0.8	5.9	6.8
7. $pK_S^0\pi^+\pi^-$	2.8	5.3	1.2	–	–	1.0	0.5	0.1	9.3	11.2
8. $\Lambda\pi^+\pi^+\pi^-$	3.0	3.0	–	2.5	–	0.9	0.8	0.8	7.9	9.4
9. $\Sigma^0\pi^+$	1.0	1.0	–	2.5	–	1.1	1.7	0.8	6.7	7.6
10.$\Sigma^+\pi^+\pi^-$	3.0	4.0	–	–	1.0	0.8	0.8	0.6	7.4	9.0

Systematic uncertainty (II): CM-energy specific

- f_{ISR} uncertainties.
  - Uncertainty of calculation algorithm: **KKMC** and **Kami**.
  - Uncertainty of input line-shape motivated by specific fit model.
  - The uncertainty of CM energy near threshold: 4574.50 ± 0.72 MeV.
  - Uncertainty of beam energy spread: $\sigma_{beam} = 1.55 \pm 0.18$ MeV.
- Uncertainties of f_{VP}.
- Uncertainties of luminosity.

$\sqrt{s}$ (GeV)	f_{ISR} (%)					f_{VP} (%)	$\mathcal{L}_{int}$ (%)
	Algorithm	Line-shape	CMS energy	Energy Spread	Total		
4.5745	3.4	1.2	18.0	3.0	18.6	0.5	–
4.580	0.7	0.6	–	0.2	0.9	0.5	0.7
4.590	0.2	1.7	–	–	1.7	0.5	0.7
4.5995	0.1	2.6	–	–	2.6	0.5	–

Total Born cross section

The Born cross section of channel i:

$$x_i = \frac{N_i}{\mathcal{L}_{\text{int.}} \cdot \varepsilon_i \cdot f_{\text{VP.}} \cdot f_{\text{ISR}} \cdot BR_i} \tag{1}$$

The total Born cross section:

$$\bar{x} = \sum_i w_i x_i,\, w_i = (1/\sigma_i^2) \Big/ \left(\sum_i 1/\sigma_i^2 \right) \tag{2}$$

and corresponding uncertainty takes the form

$$\sigma_{\bar{x}}^2 = \sum_{i,j} w_i (\mathbf{M}_x)_{ij} w_j \tag{3}$$

or approximately

$$\sigma_{\bar{x},stat.}^2 = \sum_{i,j} w_i (\mathbf{M}_x^{stat.})_{ij} w_j \quad \text{and} \quad \sigma_{\bar{x},syst.}^2 = \sum_{i,j} w_i (\mathbf{M}_x^{syst.})_{ij} w_j \tag{4}$$

The total Born cross sections:

$\sqrt{s}$(GeV)	$\mathcal{L}_{int}$ (pb^{-1})	f_{ISR}	$\sigma^{Born}_{\Lambda_c^+}$ (pb)	$\sigma^{Born}_{\bar{\Lambda}_c^-}$ (pb)	$\overline{\sigma^{Born}}$ (pb)
4.5745	47.67	0.45	$243 \pm 16 \pm 48$	$230 \pm 16 \pm 45$	$236 \pm 11 \pm 46$
4.580	8.545	0.66	$180 \pm 23 \pm 12$	$241 \pm 26 \pm 16$	$207 \pm 17 \pm 13$
4.590	8.126	0.71	$262 \pm 28 \pm 18$	$231 \pm 26 \pm 15$	$245 \pm 19 \pm 16$
4.5995	566.9	0.74	$238 \pm 4 \pm 15$	$236 \pm 4 \pm 15$	$237 \pm 3 \pm 15$

Angular distribution study

- Studied at $\sqrt{s} = 4.5745$ and 4.5995 GeV only.
- Divided the data into 10 $cos\theta$ bins.
- In each bin, combined signals from all tagged modes.
- Corrected the yields with the detection efficiency bin-by-bin.
- Combined the corrected yields from Λ_c^+ and $\bar{\Lambda}_c^-$ bins.
- The χ^2 fit on the angular distribution with shape $1 + \alpha_{\Lambda_c} \cos\theta$.

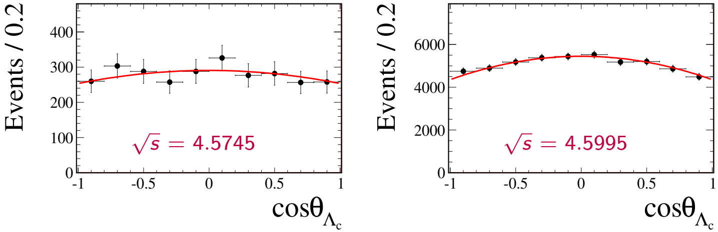

Angular distribution study

The obtained yields and detection efficiencies:

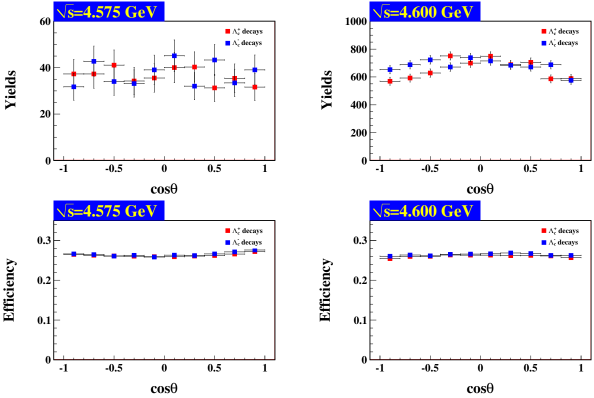

- There are 3.2% double counted events.
- Further MC study shows the affect of these events are negligible.
- The detection efficiency curve is almost flat with respect to the $\cos\theta_{\Lambda_c}$.

Angular distribution study

The Input-Output check to justify the method:

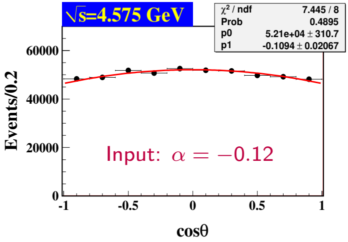

- Input the α_{Λ_c} value in simulation.
- Regarded a part of MC sample as the experimental data.
- Perform similar study procedure as in data.
- The same χ^2 fits on the angular distributions.
- The outputs are consistent with the inputs within the coverage of the uncertainty.

Angular distribution study

The systematic uncertainty of α_{Λ_c} is estimated from two aspects:

- Changing the number of bins from 10 to 20.
- Adjusting the range of the fit from (-1.0, 1.0) to (-0.8, 0.8).

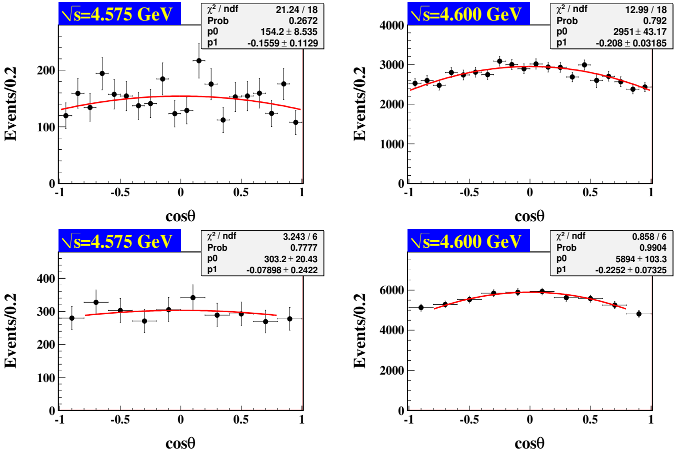

Angular distribution study

The $|G_E/G_M|$ ratios are connected with the α_{Λ_c} by following formula:

$$|G_E/G_M|^2 = (1-\alpha_{\Lambda_c})/(\frac{4m^2_{\Lambda_c^+}}{s}\alpha_{\Lambda_c} + \frac{4m^2_{\Lambda_c^+}}{s}) \tag{5}$$

The results:

$\sqrt{s}$ (GeV)	α_{Λ_c}	$\lvert G_E/G_M\rvert$
4.5745	$-0.13 \pm 0.12 \pm 0.08$	$1.14 \pm 0.14 \pm 0.07$
4.5995	$-0.20 \pm 0.04 \pm 0.02$	$1.23 \pm 0.05 \pm 0.03$

- Statistic uncertainties are dominant at both the two points.
- The systematic uncertainty of bin-by-bin efficiency correction is not considered due to the limit of the data statistic.
- This is the first time that the $|G_E/G_M|$ ratios of Λ_c are measured.

Summary

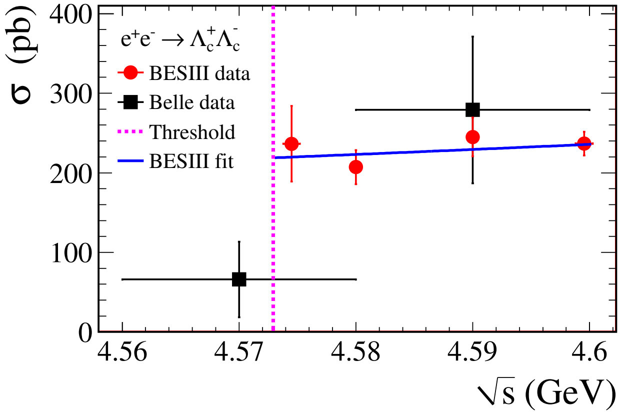

- Born cross section of $e^+e^- \to \Lambda_c^+\bar{\Lambda}_c^-$ are measured with high precision.
- The $|G_E/G_M|$ ratios of Λ_c are extracted for the first time.
- It is foreseen to obtain the phase between G_E and G_M of Λ_c.

Outlook

Mode	N^{data}	ε (%)
3. $\Lambda_c^+ \to \Lambda\pi^+$, $\Lambda \to p\pi^-$	354 ± 19	41.7
4. $\Lambda_c^- \to \bar{\Lambda}\pi^-$, $\bar{\Lambda} \to \bar{p}\pi^+$	345 ± 20	42.2

- Time-like region: EMFFs are complex with a phase.
- This is polarization effect on produced hyperon.
- In the $\Lambda_c^+ \to \Lambda\pi^+$ case, we can access to the polarization through the Λ angle and there is enough data to study this (this is why I am here).

Thanks for your attention!